

## Tailoring the second mode of Euler-Bernoulli beams: an analytical approach

Korak Sarkar\* and Ranjan Ganguli

*Department of Aerospace Engineering, Indian Institute of Science, Bangalore-560012, India*

*(Received April 1, 2014, Revised June 17, 2014, Accepted June 19, 2014)*

**Abstract.** In this paper, we study the inverse mode shape problem for an Euler-Bernoulli beam, using an analytical approach. The mass and stiffness variations are determined for a beam, having various boundary conditions, which has a prescribed polynomial second mode shape with an internal node. It is found that physically feasible rectangular cross-section beams which satisfy the inverse problem exist for a variety of boundary conditions. The effect of the location of the internal node on the mass and stiffness variations and on the deflection of the beam is studied. The derived functions are used to verify the p-version finite element code, for the cantilever boundary condition. The paper also presents the bounds on the location of the internal node, for a valid mass and stiffness variation, for any given boundary condition. The derived property variations, corresponding to a given mode shape and boundary condition, also provides a simple closed-form solution for a class of non-uniform Euler-Bernoulli beams. These closed-form solutions can also be used to check optimization algorithms proposed for modal tailoring.

**Keywords:** Euler-Bernoulli beam; free vibration; modal tailoring; inverse problem; closed-form solution

### 1. Introduction

Flexible structures like aerospace vehicles, ships, communication antennas, buildings etc. can be subjected to various kinds of excitation loads (Alshorbagy *et al.* 2011, Azizi *et al.* 2011, Bayat and Pakar 2012, Eltaher *et al.* 2012, Kisa 2012, Kural and Ozkaya 2012, Liu *et al.* 2013, Saffari *et al.* 2012, Shahba and Rajasekaran 2011, Song *et al.* 2012, Tufekci and Yigit 2012). Thus, methods for designing a structure for a desired mode shape is useful for many engineering applications, to reduce the vibrational energy from being transferred to regions where it can cause material failure. It is important to remove the vibrational energy from more sensitive parts, such as the end effector of a robotic arm, and transfer it to less sensitive regions. Hence, modal tailoring is an important problem from a structural dynamics point of view. For example, the deflections in resonant motion can be tailored to enhance the sensing abilities of capacitive resonant sensors like the microcantilever gravimetric sensor (Spletzer *et al.* 2006). Another application is the cantilevers in the Atomic Force Microscopes (AFM) where their probes can be designed for large tilts during their transversal at resonant frequency in the tapping mode (Niels 2000). In vibration control, the amplitude of vibration can be confined at certain locations as desired by the design of the mode

---

\*Corresponding author, Research Student, E-mail: korakpom@gmail.com, koraksarkar@aero.iisc.ernet.in

shapes (Gafsi *et al.* 2009).

This problem falls under the category of the “inverse mode shape problem”, which aims at determining the geometric and material data of a structure, given a certain set of mode shapes and frequencies. Barcilon (1982) developed a procedure for reconstructing the flexural rigidity and the density of a class of beam, having a free end and three different boundary conditions on the other end, from data consisting of the displacement and angle of the center line of the free left end after an initial impulse. The information content of this seismogram-like impulse response is equivalent to three spectra and two gross constants. He also discussed the conditions on the three spectra such that the flexural rigidity and density of the beam are physically meaningful. A similar work was done by Gladwell (1986), where he studied the necessary and sufficient conditions for the reconstruction of the cross-sectional area and second moment of inertia of an Euler-Bernoulli beam from the spectral data, corresponding to three end conditions. Mottershead *et al.* (2001) presented an inverse method for the assignment of natural frequencies and nodes of normal modes of vibration by the addition of grounded springs and concentrated masses. The method relies entirely on measured receptances at the coordinates of the nodes and the modifications.

Burak and Ram (2001) used a numerical technique to study the inverse problem using the knowledge of a single eigenvalue, two eigenvectors and static deflection due to unit load. Lai and Ananthasuresh (2002) solved the inverse mode shape problem with one eigenmode and all system parameters like the mass, stiffness, density, boundary conditions etc., to determine the cross-section profile for bars and beams. Ananthasuresh (2004) later extended these studies for the case of bars and beams with flexible supports. Ram and Elishakoff (2004) studied the problem for a fixed-free beam, where they used a discretized and analytical version to solve the inverse problem. Recently, Sundaram and Ananthasuresh (2013) presented a numerical solution methodology in the finite element framework for the case of bars, beams and plates to solve the inverse mode shape problem.

Enforcing nodes at selected locations is beneficial because it would allow sensitive instruments to be placed near or at nodes where there is little or no vibration. It also allows certain locations of the structure to remain stationary without rigid support. Cha and Pierre (1999) used a chain of oscillators as a means to passively impose a single node for the normal modes of any arbitrarily supported elastic structure. Cha (2002) generalized the approach to impose multiple nodes for any normal mode of an elastic structure using a set of parallel spring masses. Cha (2004, 2005) extended his theory and used tuned spring-mass oscillators to enforce nodes at any location in harmonically excited, linear elastic systems and tuned the oscillators based upon the tolerable vibration amplitudes. Cha and Zhou (2006) further expanded upon this by adding rotational oscillators, which allowed points of zero displacement and zero slope to be enforced. Cha and Chen (2011) also induced nodes along a linear structure using lumped masses alone. Cha and Rinker (2012) further extended this work by attaching properly tuned damped vibration absorbers to suppress vibration along an Euler-Bernoulli beam that includes both internal and external damping, making the problem more practical, interesting, and challenging.

Some research has used optimization methods to tailor the structural properties to obtain a targeted mode shape. Takezawa and Kitamura (2013) proposed a minimization problem using the least error between the eigenvector and target mode shape. The first and second eigenvector were considered. Numerical sensitivity and optimization analysis was used to solve the minimization problem. Maeda *et al.* (2006) proposed a topology optimization method for targeted design of structures with desired eigenfrequencies and mode shapes. The problem was motivated by the design of mechanical resonators and actuators. Rubio *et al.* (2011) mention that tailoring specified

modes is required for vibration problems. They used topology optimization and functionally graded material concepts to tailor user defined vibration nodes and solved the optimization problem using sequential linear programming. It is clear that the use of numerical optimization methods for modal tailoring is effective. However, there is a need for analytical closed form solutions to specific modal tailoring problems which can help to verify the optimization algorithms, prior to their use for design problems.

Neuringer and Elishakoff (2001) used an analytical approach using Elishakoff's method (Elishakoff 2005) to determine the mass and stiffness variations of an Euler-Bernoulli beam, given a prescribed polynomial mode shape, having an internal node. This prescribed mode shape satisfies all the boundary conditions of the beam. However, they considered only the inhomogeneous beam. They determined the elastic modulus ( $E$ ) and mass density ( $\rho$ ) of the beam as functions along the length of the beam (functionally graded materials) for the nodal placement, which poses considerable difficulty from a manufacturing point of view.

In this paper, we determine the height and breadth variations of the beam as functions along the length of the beam while keeping the elastic modulus and density of the beam as constants. These beams can be easily manufactured using Computer Numerical Control (CNC) machines, thus adding considerable practical applicability to the problem of analytically imposing an internal node. Once we determine a suitable function for the design variables given a particular mode shape and other beam parameters, we study the effect of the location of the internal node on the design variables and also the deflections of the beam. Furthermore, we try to determine the bounds on the location of the internal node. Neuringer and Elishakoff (2001) carried out their mathematical formulations considering only the pinned-pinned boundary condition. In this paper, we explore six sets of different boundary conditions and discuss them in details. Since the assumed mode shape and the corresponding mass and stiffness distributions satisfy the governing differential equations in an exact manner, they also serve as closed form solution for these beams, which can be used as test functions for approximate methods such as Rayleigh-Ritz, Galerkin and FEM. We try to verify the utility of the derived functions as benchmark solutions, for the cantilever boundary condition. They can also be used to evaluate numerical modal tailoring algorithms.

## 2. Mathematical formulation

The dynamics of a non-uniform Euler-Bernoulli beam is governed by the following fourth order differential equation (Meirovitch 1986)

$$\frac{\partial^2}{\partial x^2} \left[ EI(x) \frac{\partial^2 w(x,t)}{\partial x^2} \right] + m(x) \frac{\partial^2 w(x,t)}{\partial t^2} = 0 \quad (1)$$

where  $L$  is the length of the beam,  $EI(x)$  is the flexural rigidity of the beam,  $m(x)$  is the mass per unit length, and  $w(x,t)$  is the transverse displacement of the beam at a position  $x$ , at time  $t$ . Considering harmonic vibration, Eq. (1) yields

$$\frac{d^2}{dx^2} \left( EI(x) \frac{d^2 \phi(x)}{dx^2} \right) - m(x) \omega^2 \phi(x) = 0 \quad (2)$$

where  $\phi(x)$  and  $\omega$  denote the mode shape and frequency, respectively. We now determine a

prescribed polynomial second mode which satisfies all the boundary conditions of a given beam. Since the second mode has an internal node it is used for illustrating the mathematical approach which is generally applicable to other mode shapes. It is also possible to get the node at some pre-selected point on the beam, subject to some bounds which we will reveal later in this paper. This prescribed second mode is sought as a fifth order polynomial function given by

$$\phi(x) = c_0 + c_1x + c_2x^2 + c_3x^3 + c_4x^4 + c_5x^5 \quad (3)$$

Since Eq. (3) describes the second mode shape of a beam, it is tailored to form a node at an arbitrary position  $x = \alpha$  ( $0 < \alpha < L$ ). Using the four boundary conditions, one internal node condition  $\phi(\alpha) = 0$  and the normalization condition (in our case, mass normalization) we will have six equations, and that is why we consider the fifth order polynomial for the assumed mode shape. Our main objective is to determine a certain class of these prescribed polynomial second mode shape functions, for various boundary conditions, such that we get physically realizable variations of mass and stiffness. For our study, we take the mass distribution as a linear function of  $x$ , and the stiffness variation as a fifth order polynomial in  $x$ , given by

$$m(x) = a_0(1 + \eta x) \quad (4)$$

$$EI(x) = b_0 + b_1x + b_2x^2 + b_3x^3 + b_4x^4 + b_5x^5 \quad (5)$$

where  $\eta$ ,  $a_0$  and  $b_i$ 's are constants. Such a distribution is a good description of real structures. We put the expressions for mass and stiffness, given by Eqs. (4)-(5), and  $\phi(x)$ , given by Eq. (3), into Eq. (2), resulting in a polynomial equation with highest term of  $x^6$ . For this polynomial equation to be satisfied for all values of  $x$  ( $0 \leq x \leq L$ ), the coefficients of the constant,  $x$ ,  $x^2$ ,  $x^3$ ,  $x^4$ ,  $x^5$  and  $x^6$  must be zero. Thus yielding a set of seven linear homogeneous equations in seven unknowns.

$$\mathbf{A}y = \mathbf{0} \quad (6)$$

where  $\mathbf{A}$  is given by Eq. (A.1),  $y = (k, b_0, b_1, b_2, b_3, b_4, b_5)^T$  and  $k = \omega^2$ . To obtain a non-trivial solution for  $y$ , the determinant of  $\mathbf{A}$  must be zero, leading to a polynomial equation in  $\eta$  and  $c_i$ 's, of the form  $f(\eta, c_1, \dots, c_5) = 0$ . Solving  $f(\eta, c_1, \dots, c_5) = 0$  we will obtain the expression for  $\eta$  for which Eq. (6) will yield a non-trivial solution. We carry out our investigation for six different set of boundary conditions: cantilever, fixed-fixed, fixed-pinned, pinned-pinned, pinned-guided and fixed-guided. The different boundary conditions are shown in Table 1.

Table 1 The different boundary conditions of a non-uniform Euler-Bernoulli beam, which has been used for the second mode tailoring problem

Beam type	Boundary conditions
Cantilever	$\phi(0) = \phi'(0) = \phi''(L) = \phi'''(L) = 0$
Fixed-fixed	$\phi(0) = \phi'(0) = \phi(L) = \phi'(L) = 0$
Fixed-pinned	$\phi(0) = \phi'(0) = \phi(L) = \phi''(L) = 0$
Pinned-pinned	$\phi(0) = \phi''(0) = \phi(L) = \phi''(L) = 0$
Pinned-guided	$\phi(0) = \phi''(0) = \phi'(L) = \phi'''(L) = 0$
Fixed-guided	$\phi(0) = \phi'(0) = \phi'(L) = \phi'''(L) = 0$

### 2.1 Cantilever (Fixed-free) beam

Putting the boundary conditions of a cantilever beam, given in Table 1, along with the condition  $\phi(\alpha) = 0$  (for the internal node), into Eq. (3), and then solving for the constants  $c_i$ 's, we get

$$\begin{aligned} c_0 = 0, c_1 = 0, c_2 = -\frac{2(10L^4\alpha - 10L^3\alpha^2 + 3L^2\alpha^3)c_5}{6L^2 - 4L\alpha + \alpha^2}, \\ c_3 = \frac{2(10L^4 - 5L^2\alpha^2 + 2L\alpha^3)c_5}{6L^2 - 4L\alpha + \alpha^2}, c_4 = -\frac{(20L^3 - 10L^2\alpha + \alpha^3)c_5}{6L^2 - 4L\alpha + \alpha^2} \end{aligned} \quad (7)$$

Putting Eq. (7) into  $f(\eta, c_1, \dots, c_5) = 0$  and solving, we obtain the expression for  $\eta$ , given by Eq. (A.2). Using Eq. (A.2), we can solve Eq. (6) to get the expressions for the coefficients  $b_i$ 's in terms of  $\alpha$  and  $k$ , from which we can get the final expressions for the mass  $m(x)$  and stiffness  $EI(x)$  variations. Now, for a uniform cantilever beam, the node location for the second mode is  $\alpha = 0.783445L$ . Now, suppose we want to move this location to  $\alpha = 0.69L$ . The expressions for the assumed mode shape (normalized with respect to mass), mass and stiffness variations can be calculated as

$$\begin{aligned} \phi(x) &= -0.596661x^2 + 0.316098x^3 - 0.0512863x^4 + 0.00283851x^5 \\ m(x) &= (1 - 0.176981x)a_0 \\ EI(x) &= (0.385116 + 0.136933x + 0.0190149x^2 - 0.0220786x^3 \\ &\quad + 0.00328421x^4 - 0.000158019x^5)ka_0 \end{aligned} \quad (8)$$

We thus see that the inverse problem is solved analytically. Fig. 1(a) shows the assumed mode shapes obtained for different node locations, and their corresponding mass and stiffness variations are given in Figs. 2(a)-2(b), respectively. From Fig. 1(a), we can observe that as the node locations  $\alpha$  are shifted towards the fixed end, the amount of tip deflection increases, for a particular second mode frequency  $\omega$ , if the system is excited at the second mode frequency. This might have important applications in the MEMS industry as mechanical resonators, where we can control the amount of tip deflection by tailoring the location of the internal node.

Assuming a cantilever beam with rectangular cross-section, the height  $h(x)$  and breadth  $b(x)$  variations can be calculated as

$$h(x) = \sqrt{\frac{12 \rho EI(x)}{E m(x)}} \quad (9)$$

$$b(x) = \sqrt{\frac{E m(x)^3}{12 \rho^3 EI(x)}} \quad (10)$$

where  $\rho$  is the uniform material density and  $E$  is the elastic modulus of the beam. Taking  $L = 5$  m,  $\rho = 7840$  kg/m<sup>3</sup>,  $E = 2 \times 10^{11}$  Pa,  $\omega = 11.6642$  rad/s and  $a_0 = 1.8816$ , the height and breadth variations corresponding to two different internal node locations,  $\alpha = 0.69L$  and  $\alpha = 0.78L$ , are shown in Figs. 2(c)-2(d), respectively. For plotting purpose, the origin is taken at the center of the cross-section at the base ( $x = 0$ ). We can see the substantial difference in the beam shapes

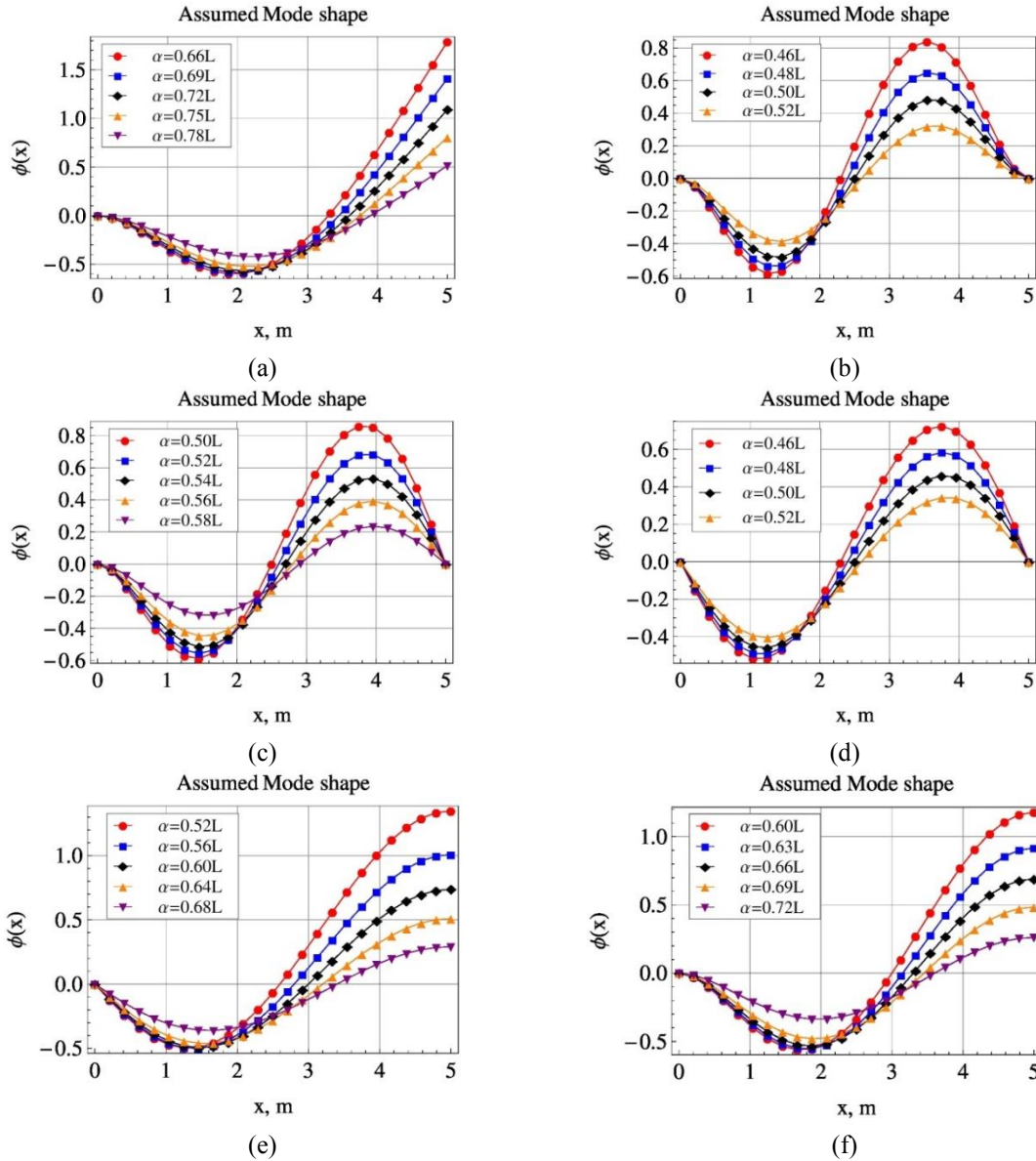


Fig. 1 The assumed mode shape variations for the beams, for different internal node locations and boundary conditions. (a) Cantilever; (b) Fixed-fixed; (c) Fixed-pinned; (d) Pinned-pinned; (e) Pinned-guided; (f) Fixed-guided

depending on the nodal placement. Conversely, the nodal point can be pre-selected by appropriate selection of the beam dimensions.

### 2.2 Fixed-fixed beam

Putting the boundary conditions of a fixed-fixed beam, given in Table 1, along with the

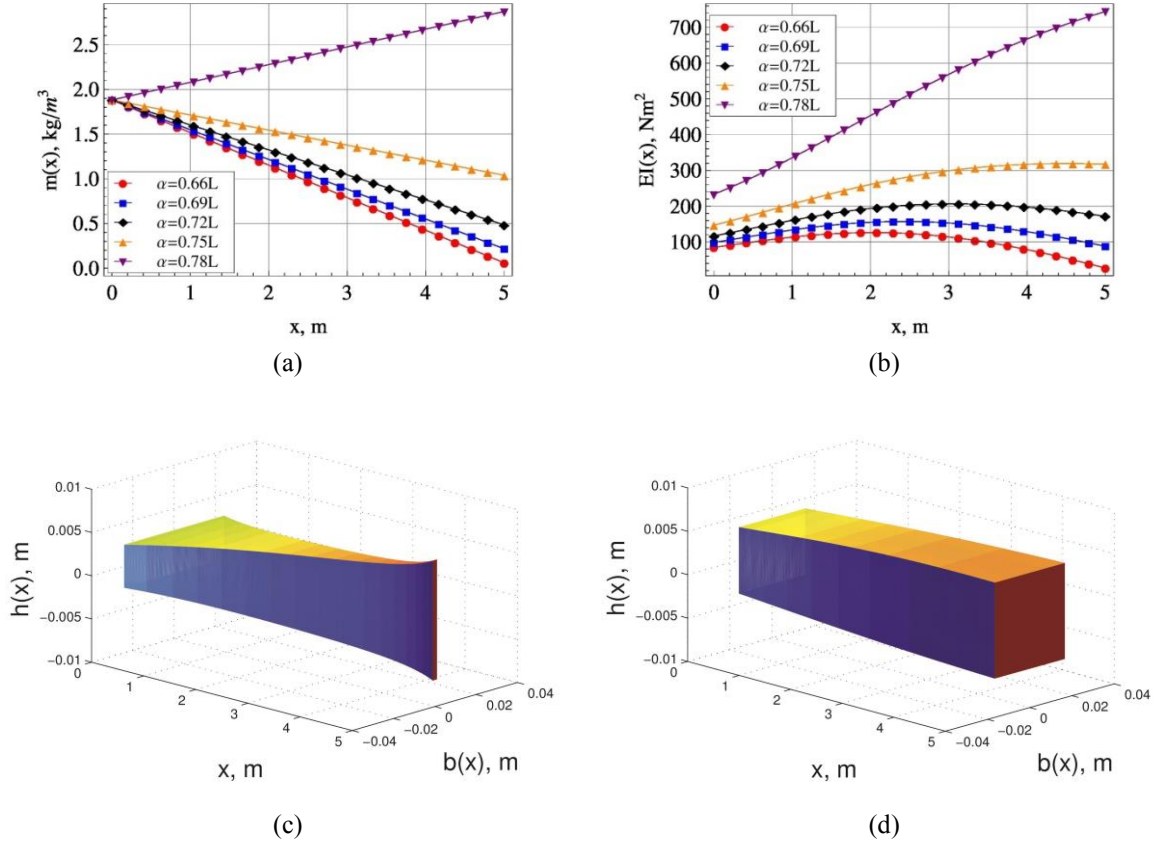


Fig. 2 Material property and geometry variations for the cantilever beam, for different internal node locations  $\alpha$ . (a) Mass variation; (b) Stiffness variation; (c) Geometry variation for  $\alpha=0.69L$ ; (d) Geometry variation for  $\alpha=0.78L$

condition  $\phi(\alpha) = 0$  (for the internal node), into Eq. (3), and then solving for the constants  $c_i$ 's, we get

$$c_0 = 0, c_1 = 0, c_2 = -L^2\alpha c_5, c_3 = L(L + 2\alpha)c_5, c_4 = -(2L + \alpha)c_5 \quad (11)$$

Putting Eq. (11) into  $f(\eta, c_1, \dots, c_5) = 0$  and solving, we obtain the expression for  $\eta$ , given by Eq. (A.3). Using Eq. (A.3), we can solve Eq. (6) to get the expressions for the coefficients  $b_i$ 's in terms of  $\alpha$  and  $k$ , from which we can get the final expressions for the mass  $m(x)$  and stiffness  $EI(x)$  variations. For a uniform fixed-fixed beam,  $\alpha = 0.5L$  for the second mode. Suppose, if we want to shift this to  $\alpha = 0.48L$ . The expressions for the assumed mode shape (normalized with respect to mass), mass and stiffness variations can be found to be

$$\begin{aligned} \phi(x) &= -1.27924x^2 + 1.04471x^3 - 0.264376x^4 + 0.0213207x^5 \\ m(x) &= (1 - 0.12896x)a_0 \\ EI(x) &= (0.0810056 + 0.0461387x + 0.0125928x^2 - 0.0128587x^3 \\ &\quad + 0.00223751x^4 - 0.000115143x^5)ka_0 \end{aligned} \quad (12)$$

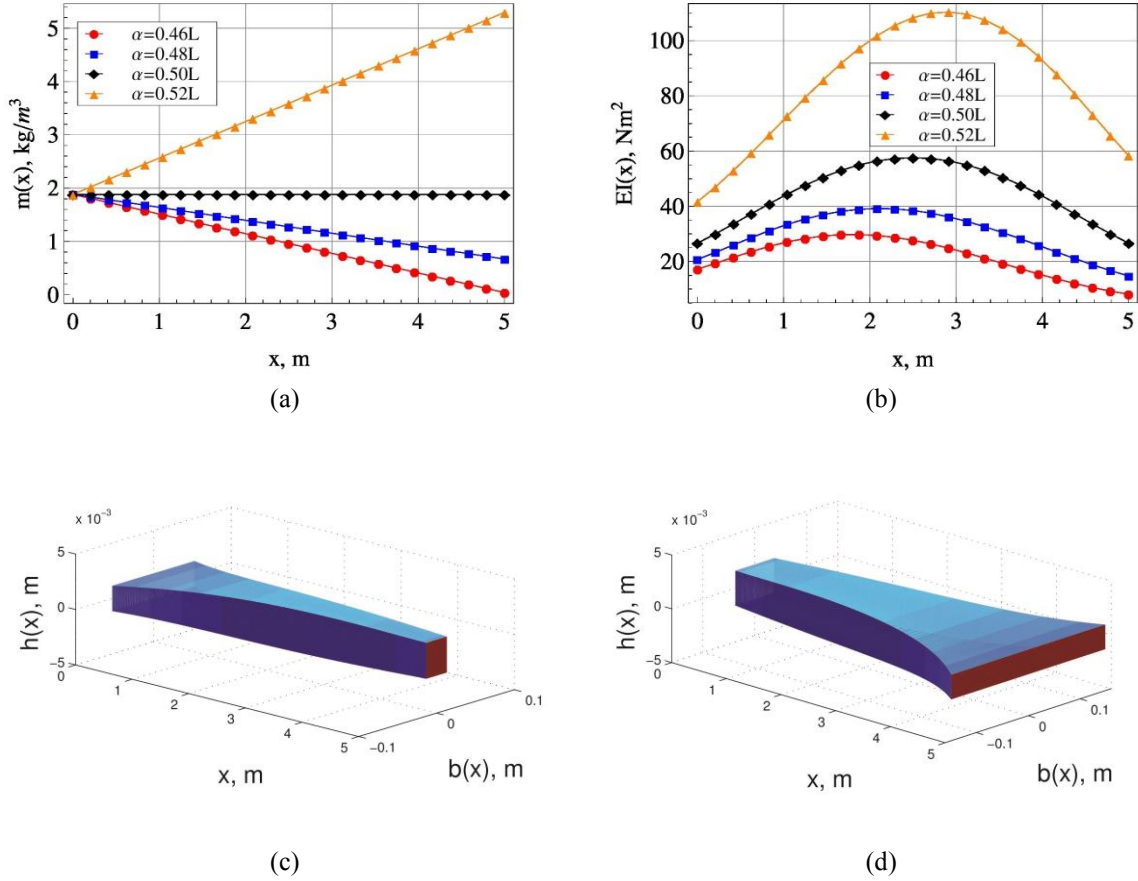


Fig. 3 Material property and geometry variations for the fixed-fixed beam, for different internal node locations  $\alpha$ . (a) Mass variation; (b) Stiffness variation; (c) Geometry variation for  $\alpha=0.48L$ ; (d) Geometry variation for  $\alpha=0.52L$

Fig. 1(b) shows the assumed mode shapes, obtained for different node locations, and their corresponding mass and stiffness variations are given in Figs. 3(a)-3(b), respectively. Taking the same values as before, the height and breadth variations corresponding to two different internal node locations,  $\alpha = 0.48L$  and  $\alpha = 0.52L$ , are shown in Figs. 3(c)-3(d), respectively.

### 2.3 Fixed-pinned beam

Putting the boundary conditions of a fixed-pinned beam, given in Table 1, along with the condition  $\phi(\alpha) = 0$  (for the internal node), into Eq. (3), and then solving for the constants  $c_i$ 's, we get

$$c_0 = 0, c_1 = 0, c_2 = -\frac{L^2(4L - 3\alpha)\alpha c_5}{3L - 2\alpha},$$

$$c_3 = \frac{L(4L^2 + 4L\alpha - 5\alpha^2)c_5}{3L - 2\alpha}, c_4 = \frac{(-7L^2 + 2L\alpha + 2\alpha^2)c_5}{3L - 2\alpha} \quad (13)$$

Putting Eq. (13) into  $f(\eta, c_1, \dots, c_5) = 0$  and solving, we obtain the expression for  $\eta$ , given by Eq. (A.4). Using Eq. (A.4), we can solve Eq. (6) to get the expressions for the constants  $b_i$ 's in terms of  $\alpha$  and  $k$ , from which we can get the final expressions for the mass  $m(x)$  and stiffness  $EI(x)$  variations. For a uniform fixed-pinned beam,  $\alpha = 0.557496L$ . Suppose, we want to move this node location to  $\alpha = 0.58L$ . The expressions for the assumed mode shape (normalized with respect to mass), mass and stiffness variations can be calculated as

$$\begin{aligned} \phi(x) &= -0.554714x^2 + 0.392549x^3 - 0.0874678x^4 + 0.00622932x^5 \\ m(x) &= (1 + 0.767163x)a_0 \\ EI(x) &= (0.342794 + 0.181087x + 0.0601321x^2 - 0.00516956x^3 \\ &\quad - 0.0058626x^4 + 0.000684967x^5)ka_0 \end{aligned} \tag{14}$$

Fig. 1(c) shows the assumed mode shapes, obtained for different node locations, and their corresponding mass and stiffness variations are given in Figs. 4(a)-4(b), respectively. Taking the same values as before, the height and breadth variations corresponding to two different internal node locations,  $\alpha = 0.52L$  and  $\alpha = 0.58L$ , are shown in Figs. 4(c)-4(d), respectively.

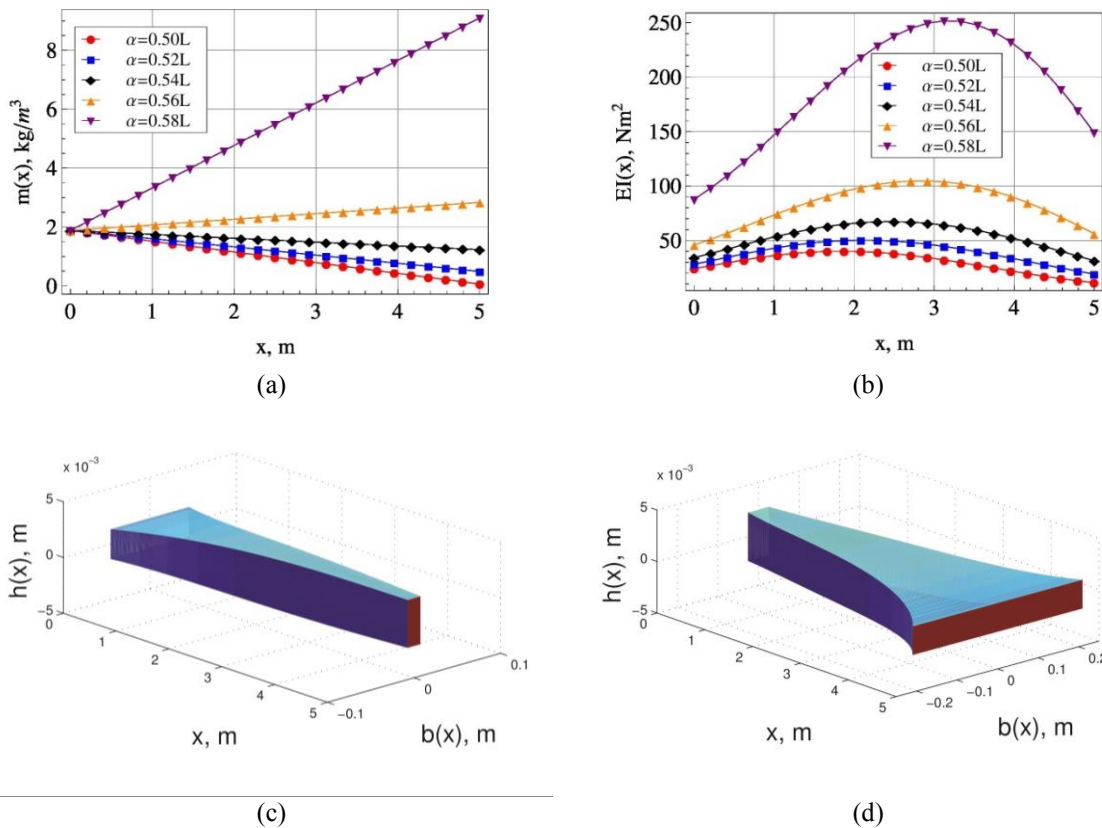


Fig. 4 Material property and geometry variations for the fixed-pinned beam, for different internal node locations  $\alpha$ . (a) Mass variation; (b) Stiffness variation; (c) Geometry variation for  $\alpha=0.52L$ ; (d) Geometry variation for  $\alpha=0.58L$

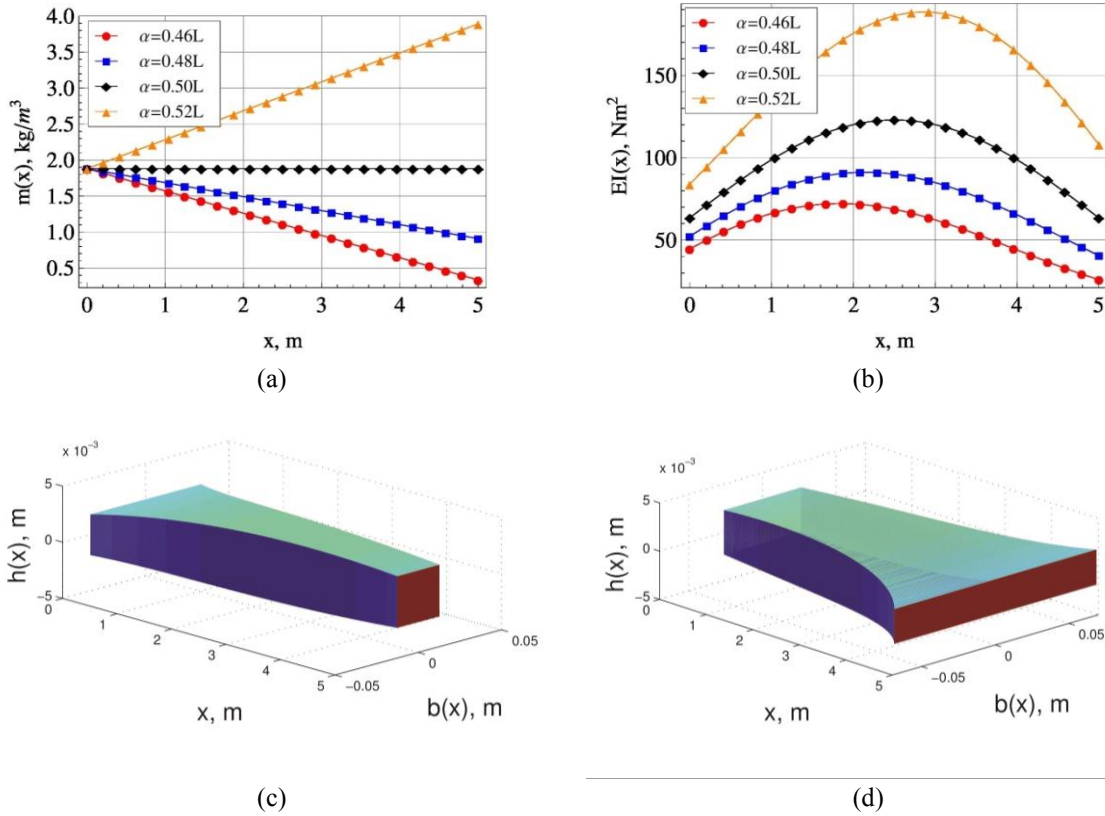


Fig. 5 Material property and geometry variations for the pinned-pinned beam, for different internal node locations  $\alpha$ . (a) Mass variation; (b) Stiffness variation; (c) Geometry variation for  $\alpha=0.48L$ ; (d) Geometry variation for  $\alpha=0.52L$

## 2.4 Pinned-pinned beam

Putting the boundary conditions of a pinned-pinned beam, given in Table 1, along with the condition  $\phi(\alpha) = 0$  (for the internal node), into Eq. (3), and then solving for the constants  $c_i$ 's, we get

$$c_0 = 0, c_1 = \frac{L^3 \alpha^2 (-4L + 3\alpha) c_5}{3(L^2 + L\alpha - \alpha^2)}, c_2 = 0, c_3 = \frac{2L(2L^3 + 2L^2\alpha + 2L\alpha^2 - 3\alpha^3) c_5}{3(L^2 + L\alpha - \alpha^2)},$$

$$c_4 = \frac{(-7L^3 - 7L^2\alpha + 3L\alpha^2 + 3\alpha^3) c_5}{3(L^2 + L\alpha - \alpha^2)} \quad (15)$$

Putting Eq. (15) into  $f(\eta, c_1, \dots, c_5) = 0$  and solving, we obtain the expression for  $\eta$ , given by Eq. (A.5). Using Eq. (A.5), we can solve Eq. (6) to get the expressions for the constants  $b_i$ 's in terms of  $\alpha$  and  $k$ , from which we can get the final expressions for the mass  $m(x)$  and stiffness  $EI(x)$  variations. For a uniform pinned-pinned beam, the node location for the second mode is  $\alpha = 0.5L$ . Suppose, we want to move this node to  $\alpha = 0.48L$ . The expressions for the assumed mode shape (normalized with respect to mass), mass and stiffness variations can be found to be

$$\begin{aligned}
\phi(x) &= -0.692524x + 0.290151x^3 - 0.0877022x^4 + 0.00704246x^5 \\
m(x) &= (1 - 0.103282x)a_0 \\
EI(x) &= (0.204178 + 0.123432x - 0.0082004x^2 - 0.01152x^3 \\
&\quad + 0.00203263x^4 - 0.0000922157x^5)ka_0
\end{aligned} \tag{16}$$

Fig. 1(d) shows the assumed mode shapes, obtained for different node locations, and their corresponding mass and stiffness variations are given in Figs. 5(a)-5(b), respectively. Taking the same values as before, the height and breadth variations corresponding to two different internal node locations,  $\alpha = 0.48L$  and  $\alpha = 0.52L$ , are given in Figs. 5(c)-5(d), respectively.

### 2.5 Pinned-guided beam

Putting the boundary conditions of a pinned-guided beam, given in Table 1, along with the condition  $\phi(\alpha) = 0$  (for the internal node), into Eq. (3), and then solving for the constants  $c_i$ 's, we get

$$\begin{aligned}
c_0 = 0, c_1 &= \frac{L^3\alpha^2(-20L^2 + 25L\alpha - 8\alpha^2)c_5}{8L^3 - 4L\alpha^2 + \alpha^3}, c_2 = 0, c_3 = \frac{2L(10L^4 - 5L\alpha^3 + 2\alpha^4)c_5}{8L^3 - 4L\alpha^2 + \alpha^3}, \\
c_4 &= -\frac{(-5L^2 + \alpha^2)^2c_5}{8L^3 - 4L\alpha^2 + \alpha^3}
\end{aligned} \tag{17}$$

Putting Eq. (17) into  $f(\eta, c_1, \dots, c_5) = 0$  and solving, we obtain the expression for  $\eta$ , given by Eq. (A.6). Using Eq. (A.6), we can solve Eq. (6) to get the expressions for the constants  $b_i$ 's in terms of  $\alpha$  and  $k$ , from which we can get the final expressions for the mass  $m(x)$  and stiffness  $EI(x)$  variations. For a uniform pinned-guided beam,  $\alpha = 0.666667L$ . Now, suppose we want to move the node location to  $\alpha = 0.56L$ . The expressions for the assumed mode shape (normalized with respect to mass), mass and stiffness variations can be calculated as

$$\begin{aligned}
\phi(x) &= -0.579998x + 0.16204x^3 - 0.0381901x^4 + 0.00240705x^5 \\
m(x) &= (1 - 0.173596x)a_0 \\
EI(x) &= (0.412504 + 0.19444x - 0.0281992x^2 - 0.0142899x^3 \\
&\quad + 0.00299386x^4 - 0.000154996x^5)ka_0
\end{aligned} \tag{18}$$

Fig. 1(e) shows the assumed mode shapes, obtained for different node locations, and their corresponding mass and stiffness variations are given in Figs. 6(a)-6(b), respectively. Taking the same values as before, the height and breadth variations corresponding to two different internal node locations,  $\alpha = 0.56L$  and  $\alpha = 0.68L$ , are shown in Figs. 6(c)-6(d), respectively. From Fig. 1(e), we can observe that by shifting the internal node location towards the pinned end, the deflection at the guided end of the beam increases, if the system is excited at the second mode frequency.

### 2.6 Fixed-guided beam

Putting the boundary conditions of a fixed-guided beam, given in Table 1, along with the

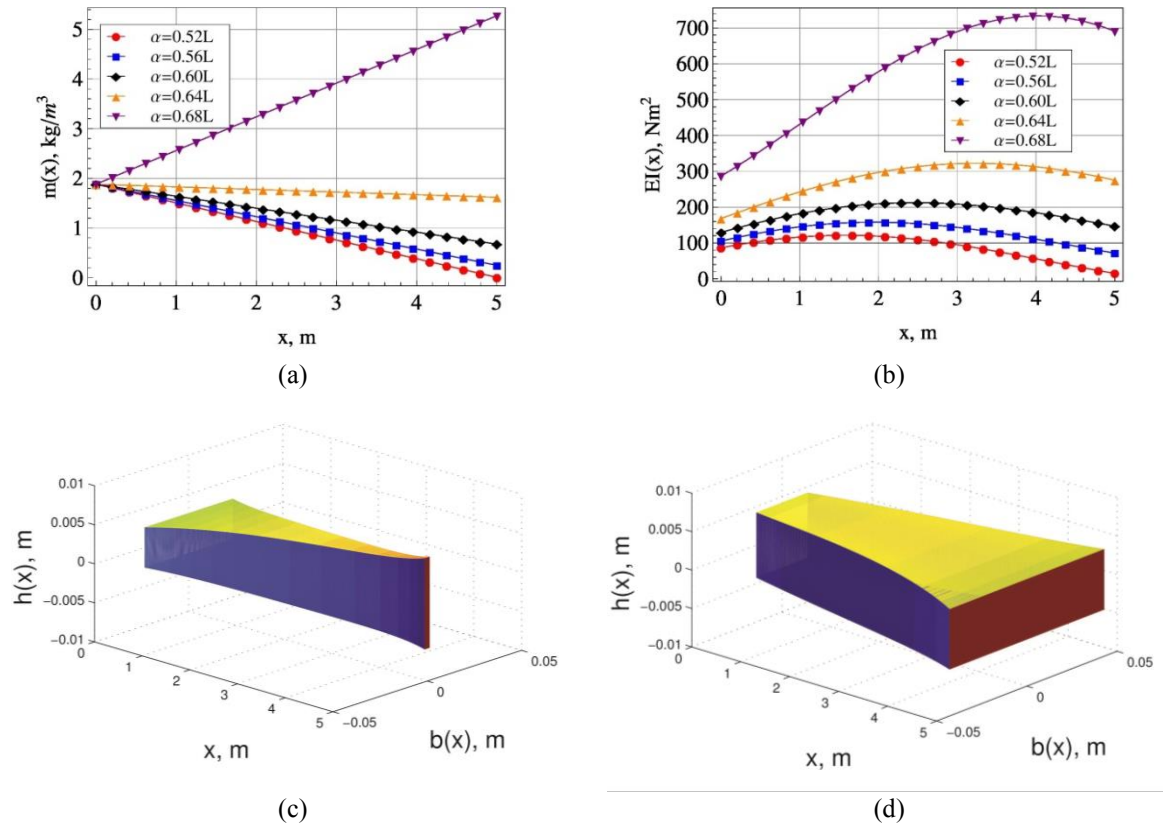


Fig. 6 Material property and geometry variations for the pinned-guided beam, for different internal node locations  $\alpha$ . (a) Mass variation; (b) Stiffness variation; (c) Geometry variation for  $\alpha=0.56L$ ; (d) Geometry variation for  $\alpha=0.68L$

condition  $\phi(\alpha) = 0$  (for the internal node), into Eq. (3), and then solving for the constants  $c_i$ 's, we get

$$c_0 = 0, c_1 = 0, c_2 = \frac{L^2\alpha(-20L^2 + 25L\alpha - 8\alpha^2)c_5}{2(-2L + \alpha)^2}, c_3 = \frac{2L(5L^3 - 5L\alpha^2 + 2\alpha^3)c_5}{(-2L + \alpha)^2},$$

$$c_4 = \frac{(-25L^3 + 20L^2\alpha - 2\alpha^3)c_5}{2(-2L + \alpha)^2} \tag{19}$$

Putting Eq. (19) into  $f(\eta, c_1, \dots, c_5) = 0$  and solving, we obtain the expression for  $\eta$ , given by Eq. (A.7). Using Eq. (A.7), we can solve Eq. (6) to get the expressions for the constants  $b_i$ 's in terms of  $\alpha$  and  $k$ , from which we can get the final expressions for the mass  $m(x)$  and stiffness  $EI(x)$  variations. For a uniform fixed-guided beam,  $\alpha = 0.716806L$ . Suppose, we want to move the node to  $\alpha = 0.63L$ . The expressions for the assumed mode shape (normalized with respect to mass), mass and stiffness variations can be found to be

$$\phi(x) = -0.720588x^2 + 0.433239x^3 - 0.0794862x^4 + 0.00462594x^5$$

$$m(x) = (1 - 0.16011x)a_0$$

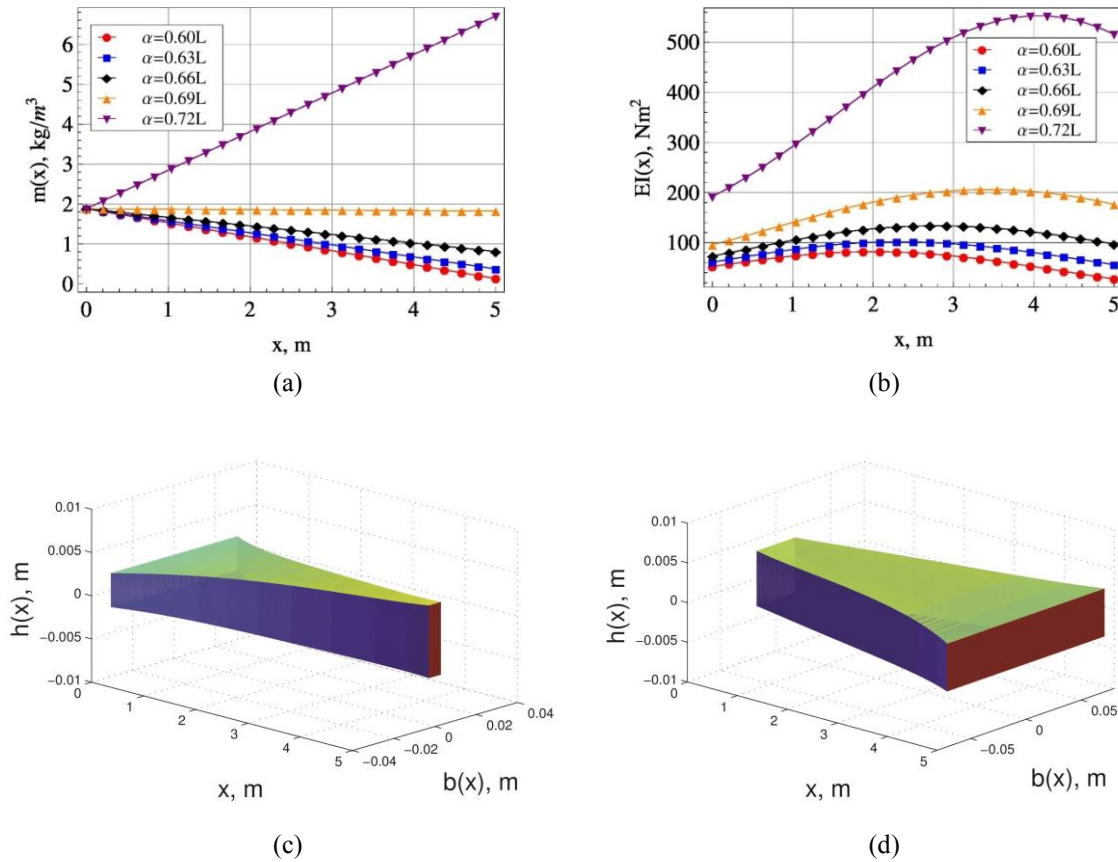


Fig. 7 Material property and geometry variations for the fixed-guided beam, for different internal node locations  $\alpha$ . (a) Mass variation; (b) Stiffness variation; (c) Geometry variation for  $\alpha=0.63L$ ; (d) Geometry variation for  $\alpha=0.72L$

$$EI(x) = (0.239388 + 0.0971021x + 0.0167046x^2 - 0.0187686x^3 + 0.00299181x^4 - 0.000142956x^5)ka_0 \tag{20}$$

Fig. 1(f) shows the assumed mode shapes, obtained for different node locations, and their corresponding mass and stiffness variations are given in Figs. 7(a)-7(b), respectively. Taking the same values as before, the height and breadth variations corresponding to two different internal node locations,  $\alpha = 0.63L$  and  $\alpha = 0.72L$ , are shown in Figs. 7(c)-7(d), respectively. Here also we can observe from Fig. 1(f), that by shifting the location of the internal node towards the fixed end, the deflection at the guided end of the beam increases, if the system is excited with the second mode frequency.

### 3. Validation of derived functions using p-version finite element method

The finite element is one of the most popular methods used for the vibration analysis of beams.

Most of the early works have used the Hermite cubic polynomial as shape functions, which is known as the h-version finite element method (Udupa and Varadan 1990). This method works well for uniform beams, but for non-uniform beams a large number of elements are required for the convergence of results. Hence in later years new types of finite element methods were developed which use only one element like the p-version (Hodges and Rutkowski 1981), Fourier-p super element (Gunda *et al.* 2007) and spectral methods (Vinod *et al.* 2007).

The  $EI(x)$  variations, derived for the various distributions of mass per unit length  $m(x)$ , can be used as test functions for checking the validity of these beam finite element methods, by comparing the known fundamental frequency  $\omega$  and mode shape  $\phi(x)$  with that derived from the numerical code. In our case, we use the p-version of the finite element introduced by Hodges and Rutkowski (1981). This method is very popular, not only because it is highly efficient in handling non-uniform structures, but also because it reduces the order of the eigenvalue problem to a great extent, since it uses increased order of the polynomial basis for convergence of results. A detailed formulation of the method is given by Sarkar and Ganguli (2013), the only difference being the expression for the axial tension force term  $T(x)$ . For rotating beams it is  $T(x) = \int_x^L m(x)\Omega^2 x dx$ , where  $\Omega$  is the rotating speed for the rotating beam. For our case  $T(x) = 0$ .

As an example, we take the mass and stiffness variations derived for the cantilever boundary condition, shown in Figs. 2(a)-2(b), respectively, and put them into the p-version finite element method to obtain the second mode shape and frequency. The results are then compared with the assumed mode shape  $\phi(x)$  and frequency  $\omega$ . The reason for finding the second mode frequency is that our assumed mode shape has an internal node present, and hence it represents the second elastic mode of a cantilever beam. The results for the mode shape comparisons are shown in Fig. 8. All the mode shapes have been mass normalized. The second mode frequency yielded by p-FEM, for different positions of the internal nodes, came as 11.6642 rad/s, which is the same as assumed in Section 2.1. Thus we can see that the test functions, for the cantilever beam, give back the same frequency  $\omega$  and mode shape  $\phi(x)$  as we had assumed in the Section 2.1. Indirectly, it also checked the correctness of the derived functions.

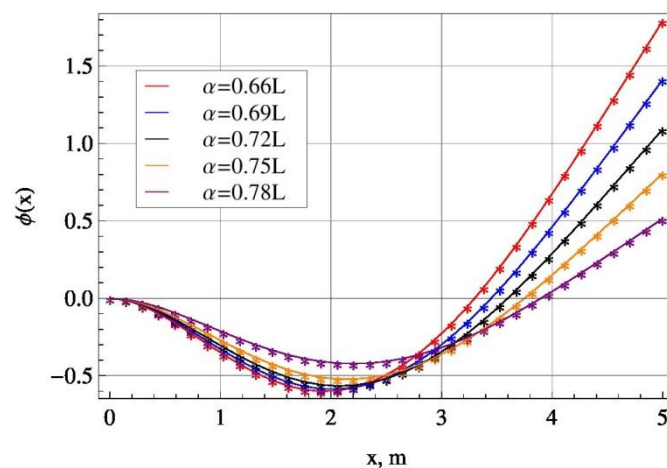


Fig. 8 Comparison of the assumed fundamental mode shapes and mode shapes obtained from p-FEM, for the case of a cantilever second mode, for different positions of the internal node  $\alpha$ . “\*” denotes mode shapes obtained from the p-FEM, continuous lines denotes the assumed mode shapes

Table 2 The bounds on the location of the internal node ( $\alpha$ ), for different boundary conditions, along with the values of  $\alpha$  for corresponding uniform beams and  $\eta=0$ . All values are given as a fraction of the total beam span

Beam type	Bounds on the internal node $\alpha$	$\alpha$ location for corresponding uniform beam	$\alpha$ for which $\eta=0$
Cantilever	$0.644294 < \alpha < 0.806105$	0.783445	0.769396
Fixed-fixed	$0.458307 < \alpha < 0.541693$	0.5	0.5
Fixed-pinned	$0.496157 < \alpha < 0.593685$	0.557496	0.550426
Pinned-pinned	$0.442801 < \alpha < 0.557199$	0.5	0.5
Pinned-guided	$0.518617 < \alpha < 0.708167$	0.66667	0.646348
Fixed-guided	$0.574623 < \alpha < 0.735808$	0.716806	0.690983

#### 4. Bounds on the location of the internal node

Till now we have seen that it is possible to shift the location of the internal node of the second mode of an Euler-Bernoulli beam, having different boundary conditions, by appropriately varying the mass and stiffness of the beam. But one question that immediately arises - can the location of the internal node be shifted to anywhere along the length of the beam? The obvious answer is no. This leads us to investigate the bounds on the locations of the internal node for all the given set of boundary conditions.

In formulating the problem for the six different boundary conditions, we have seen that for non-trivial solutions to exist, there arises a specific relation between the constant  $\eta$  and the internal node location  $\alpha$ , given by Eqs. (A.2)-(A.7). But the constant  $\eta$  cannot be less than  $-1$ , otherwise the mass variation will become negative, which is not allowable from a physical point of view. Hence, we have

$$m(x) > 0 \forall x, 0 \leq x \leq L \Rightarrow \eta > -1 \quad (21)$$

Thus, imposing the condition given by Eqn. (21), on the  $\eta$  expressions derived for the different boundary conditions, we can get a bound on the values of the internal node  $\alpha$ . The calculation is done by a simple MATHEMATICA code, and the results for the different boundary conditions are presented in Table 2.

Another interesting observation that we can make from Figs. (2), (3), (4), (5), (6) & (7), is that for a particular location of the internal node, the mass distribution becomes constant, that is the value of  $\eta$  becomes zero. Thus, the values of the corresponding  $\alpha$ 's for which  $\eta = 0$ , can be calculated using Eqs. (A.2)-(A.7), respectively, and the results are tabulated in Table 2, along with the location of the internal node for the corresponding uniform beams.

#### 4. Conclusions

In this paper, we have given an analytical approach for tailoring the second mode of an Euler-Bernoulli beam, having different boundary conditions. The approach allows pre-selection of a nodal location in the beam for the second mode. We assume a certain mode shape function  $\phi(x)$ , having an internal node at  $x = \alpha$ , which satisfies all the given boundary conditions. We then assume the mass distribution  $m(x)$  to vary linearly with  $x$  and the flexural stiffness  $EI(x)$  to vary as a fifth

order polynomial in  $x$ . Putting  $\phi(x)$ ,  $m(x)$  &  $EI(x)$  into the governing differential equations, and arguing that since solution must exist for all values of  $x$ , we form seven linear equations in seven unknowns. Invoking the conditions for non-trivial solutions, we determine the relation between the mass slope  $\eta$  and internal node  $\alpha$ , from which we can get the final expressions for the mass and flexural stiffness variations.

The variations of the mass and stiffness distributions corresponding to different locations of the internal node have been shown, for six different sets of boundary conditions. We also concluded that by shifting the location of the internal node we can change the degree of deflection of the beam when excited with a frequency  $\omega$ . Hence, if we assume the second natural frequency as  $\omega$ , then we can tailor the mass and stiffness variations accordingly, for a particular location of the node. Hence these results also serve as simple closed-form solution to the governing differential equation of the beam, which can be used as test functions for validating numerical methods of vibration tailoring. We used the derived functions for the cantilever boundary condition, to validate the p-version finite element method, thus proving the utility of the derived functions as benchmark solutions. Furthermore, we also calculated the bounds on the location of the internal node for the different type of beams. Thus, the results can be used to tailor Euler-Bernoulli beams having a prescribed second mode shape with a particular node location, corresponding to the second natural frequency  $\omega$ .

## References

- Alshorbagy, A., Eltaher, M. and Mahmoud, F. (2011), "Free vibration characteristics of a functionally graded beam by finite element method", *Appl. Math. Model.*, **35**(1), 412-425.
- Ananthasuresh, G. (2004), "Inverse mode shape problems for bars and beams with flexible supports", *Inverse Problems, Design and Optimization Symposium*, Rio de Janeiro, Brazil.
- Azizi, N., Saadatpour, M. and Mahzoon, M. (2011), "Using spectral element method for analyzing continuous beams and bridges subjected to a moving load", *Appl. Math. Model.*, **36**(8), 3580-3592.
- Barcilon, V. (1982), "Inverse problem for the vibrating beam in the free-clamped configuration", *Philos. T. Roy. Soc. A*, **304**(1483), 211-251.
- Bayat, M. and Pakar, I. (2012), "Accurate analytical solution for nonlinear free vibration of beams", *Struct. Eng. Mech.*, **43**(3), 337-347.
- Burak, S. and Ram, Y. (2001), "The construction of physical parameters from modal data", *Mech. Syst. Signal Pr.*, **15**(1), 3-10.
- Cha, P. (2002), "Specifying nodes at multiple locations for any normal mode of a linear elastic structure", *J. Sound Vib.*, **250**(5), 923-934.
- Cha, P. (2004), "Imposing nodes at arbitrary locations for general elastic structures during harmonic excitations", *J. Sound Vib.*, **272**(3), 853-868.
- Cha, P. (2005), "Enforcing nodes at required locations in a harmonically excited structure using simple oscillators", *J. Sound Vib.*, **279**(3), 799-816.
- Cha, P. and Chen, C. (2011), "Quenching vibration along a harmonically excited linear structure using lumped masses", *J. Vib. Control*, **17**(4), 527-539.
- Cha, P. and Pierre, C. (1999), "Imposing nodes to the normal modes of a linear elastic structure", *J. Sound Vib.*, **219**(4), 669-687.
- Cha, P. and Rinker, J. (2012), "Enforcing nodes to suppress vibration along a harmonically forced damped Euler-Bernoulli beam", *J. Vib. Acoust.*, **134**(5), 051010-051019.
- Cha, P. and Zhou, X. (2006), "Imposing points of zero displacements and zero slopes along any linear structure during harmonic excitations", *J. Sound Vib.*, **297**(1), 55-71.

- Elishakoff, I. (2005), *Eigenvalues Of Inhomogeneous Structures: Unusual Closed-form Solutions*, CRC Press, Boca Raton, Florida, USA.
- Eltaher, M., Alshorbagy, A. and Mahmoud, F. (2012), "Vibration analysis of Euler-Bernoulli nanobeams by using finite element method", *Appl. Math. Model.*, **37**(7), 4787-4797.
- Gafsi, W., Choura, S. and Nayfeh, A. (2009), "Assignment of geometrical and physical parameters for the confinement of vibrations in flexible structures", *J. Aerospace Eng.*, **22**(4), 403-414.
- Gladwell, G. (1986), "The inverse problem for the Euler-Bernoulli beam", *P. Roy. Soc. Lond. A Mat.*, **407**(1832), 199-218.
- Gunda, J.B., Singh, A.P., Chhabra, P.S. and Ganguli, R. (2007), "Free vibration analysis of rotating tapered blades using Fourier-p super element", *Struct. Eng. Mech.*, **27**(2), 243-257.
- Hodges, D. Y. and Rutkowski, M. Y. (1981), "Free-vibration analysis of rotating beams by a variable-order finite-element method", *AIAA J.*, **19**(11), 1459-1466.
- Kisa, M. (2012), "Vibration and stability of axially loaded cracked beams", *Struct. Eng. Mech.*, **44**(3), 305-323.
- Kural, S. and Ozkaya, E. (2012), "Vibrations of an axially accelerating, multiple supported flexible beam", *Struct. Eng. Mech.*, **44**(4), 521-538.
- Lai, E. and Ananthasuresh, G. (2002), "On the design of bars and beams for desired mode shapes", *J. Sound Vib.*, **254**(2), 393-406.
- Liu, Z., Yin, Y., Wang, F., Zhao, Y. and Cai, L. (2013), "Study on modified differential transform method for free vibration analysis of uniform Euler-Bernoulli beam", *Struct. Eng. Mech.*, **48**(5), 697-709.
- Maeda, Y., Nishiwaki, S., Izui, K., Yoshimura, M., Matsui, K. and Terada, K. (2006), "Structural topology optimization of vibrating structures with specified eigenfrequencies and eigenmode shapes", *Int. J. Numer. Meth. Eng.*, **67**(5), 597-628.
- Meirovitch, L. (1986), *Elements Of Vibration Analysis*, Vol. 2, McGraw-Hill, New York.
- Mottershead, J., Mares, C. and Friswell, M. (2001), "An inverse method for the assignment of vibration nodes", *Mech. Syst. Signal Pr.*, **15**(1), 87-100.
- Neuringer, J. and Elishakoff, I. (2001), "Inhomogeneous beams that may possess a prescribed polynomial second mode", *Chaos Soliton. Fract.*, **12**(5), 881-896.
- Niels, L. (2000), "Design of cantilever probes for atomic force microscopy (AFM)", *Eng. Optimiz.*, **32**(3), 373-392.
- Ram, Y. and Elishakoff, I. (2004), "Reconstructing the cross-sectional area of an axially vibrating non-uniform rod from one of its mode shapes", *P. Roy. Soc. Lond. A Mat.*, **460**(2046), 1583-1596.
- Rubio, W., Paulino, G. and Silva, E. (2011), "Tailoring vibration mode shapes using topology optimization and functionally graded material concepts", *Smart Mater. Struct.*, **20**(2), 025009.
- Saffari, H., Mohammadnejad, M. and Bagheripour, M. (2012), "Free vibration analysis of non-prismatic beams under variable axial forces", *Struct. Eng. Mech.*, **43**(5), 561-582.
- Sarkar, K. and Ganguli, R. (2013), "Rotating beams and non-rotating beams with shared eigenpair for pinned-free boundary condition", *Meccanica*, **48**(7), 1661-1676.
- Shahba, A. and Rajasekaran, S. (2011), "Free vibration and stability of tapered Euler-Bernoulli beams made of axially functionally graded materials", *Appl. Math. Model.*, **36**(7), 3094-3111.
- Song, Z., Li, W. and Liu, G. (2012), "Stability and non-stationary vibration analysis of beams subjected to periodic axial forces using discrete singular convolution", *Struct. Eng. Mech.*, **44**(4), 487-499.
- Spletzer, M., Raman, A., Wu, A., Xu, X. and Reifenberger, R. (2006), "Ultrasensitive mass sensing using mode localization in coupled microcantilevers", *Appl. Phys. Lett.*, **88**(25), 254102-254102.
- Sundaram, M.M. and Ananthasuresh, G. (2013), "A note on the inverse mode shape problem for bars, beams, and plates", *Inverse Prob. Sci. Eng.*, **21**(1), 1-16.
- Takezawa, A. and Kitamura, M. (2013), "Sensitivity analysis and optimization of vibration modes in continuum systems", *J. Sound Vib.*, **332**(6), 1553-1566.
- Tufekci, E. and Yigit, O.O. (2012), "Effects of geometric parameters on in-plane vibrations of two-stepped circular beams", *Struct. Eng. Mech.*, **42**(2), 131-152.
- Udapa, K.M. and Varadan, T.K. (1990). Hierarchical finite element method for rotating beams", *J. Sound*

*Vib.*, **138**(3), 447-456.

Vinod, K.G., Gopalakrishnan, S. and Ganguli, R. (2007), "Free vibration and wave propagation analysis of uniform and tapered rotating beams using spectrally formulated finite elements", *Int. J. Solids Struct.*, **44**(18), 5875-5893.

## Appendix A

The expression for  $\mathbf{A}$  in Eq. (6) is given by

$$\mathbf{A} = \begin{pmatrix} -a_0c_0 & 24c_4 & 12c_3 & 4c_2 & 0 & 0 & 0 \\ -\eta a_0c_0 - a_0c_1 & 120c_5 & 72c_4 & 36c_3 & 12c_2 & 0 & 0 \\ -\eta a_0c_1 - a_0c_2 & 0 & 240c_5 & 144c_4 & 72c_3 & 24c_2 & 0 \\ -\eta a_0c_2 - a_0c_3 & 0 & 0 & 400c_5 & 240c_4 & 120c_3 & 40c_2 \\ -\eta a_0c_3 - a_0c_4 & 0 & 0 & 0 & 600c_5 & 360c_4 & 180c_3 \\ -\eta a_0c_4 - a_0c_5 & 0 & 0 & 0 & 0 & 840c_5 & 504c_4 \\ -\eta a_0c_5 & 0 & 0 & 0 & 0 & 0 & 1120c_5 \end{pmatrix} \quad (\text{A. 1})$$

The derived expression for  $\eta$ , for cantilever (fixed-free) boundary condition, is given by

$$\begin{aligned} \eta = & -(80(129600000L^{17} - 734400000L^{16}\alpha + 1884600000L^{15}\alpha^2 - 2920800000L^{14}\alpha^3 \\ & + 3059000000L^{13}\alpha^4 - 2289200000L^{12}\alpha^5 + 1263450000L^{11}\alpha^6 - 528820000L^{10}\alpha^7 \\ & + 177950000L^9\alpha^8 - 55682000L^8\alpha^9 + 19344500L^7\alpha^{10} - 7112000L^6\alpha^{11} \\ & + 2260100L^5\alpha^{12} - 546000L^4\alpha^{13} + 94175L^3\alpha^{14} - 10962L^2\alpha^{15} + 783L\alpha^{16} - 27\alpha^{17}))/ \\ & (8343000000L^{18} - 46602000000L^{17}\alpha + 118098000000L^{16}\alpha^2 \\ & - 180894000000L^{15}\alpha^3 + 187344250000L^{14}\alpha^4 - 138649500000L^{13}\alpha^5 \\ & + 75393450000L^{12}\alpha^6 - 30368400000L^{11}\alpha^7 + 8836312500L^{10}\alpha^8 - 1541595000L^9\alpha^9 \\ & - 146090000L^8\alpha^{10} + 282425000L^7\alpha^{11} - 153446625L^6\alpha^{12} + 55651750L^5\alpha^{13} \\ & - 14415875L^4\alpha^{14} + 2635500L^3\alpha^{15} - 324945L^2\alpha^{16} + 24570L\alpha^{17} - 891\alpha^{18}) \quad (\text{A. 2}) \end{aligned}$$

The derived expression for  $\eta$ , for fixed-fixed boundary condition, is given by

$$\eta = \frac{-71040L^5 + 118400L^4\alpha + 62400L^3\alpha^2 - 12800L^2\alpha^3 - 43200L\alpha^4 + 17280\alpha^5}{34473L^6 - 45266L^5\alpha - 33650L^4\alpha^2 - 9440L^3\alpha^3 + 11700L^2\alpha^4 + 12744L\alpha^5 - 7128\alpha^6} \quad (\text{A. 3})$$

The derived expression for  $\eta$ , for fixed-pinned boundary condition, is given by

$$\begin{aligned} \eta = & -(320(-2L + \alpha)^2(77679L^9 - 362502L^8\alpha + 611847L^7\alpha^2 - 431880L^6\alpha^3 \\ & + 81082L^5\alpha^4 - 6452L^4\alpha^5 + 86596L^3\alpha^6 - 81216L^2\alpha^7 + 28080L\alpha^8 - 3456\alpha^9))/ \\ & (55190808L^{12} - 298001808L^{11}\alpha + 641850372L^{10}\alpha^2 - 701769480L^9\alpha^3 \\ & + 404906750L^8\alpha^4 - 121263668L^7\alpha^5 + 21954633L^6\alpha^6 + 21437998L^5\alpha^7 \\ & - 58309060L^4\alpha^8 + 52463400L^3\alpha^9 - 23165568L^2\alpha^{10} + 5125248L\alpha^{11} - 456192\alpha^{12}) \quad (\text{A. 4}) \end{aligned}$$

The derived expression for  $\eta$ , for pinned-pinned boundary condition, is given by

$$\begin{aligned} \eta = & -(20(7672L^{17} + 46032L^{16}\alpha + 8668L^{15}\alpha^2 - 333335L^{14}\alpha^3 \\ & - 317555L^{13}\alpha^4 + 846457L^{12}\alpha^5 + 839737L^{11}\alpha^6 - 1261667L^{10}\alpha^7 \end{aligned}$$

$$\begin{aligned}
& -890775L^9\alpha^8 + 1214845L^8\alpha^9 + 370557L^7\alpha^{10} - 688293L^6\alpha^{11} + 18603L^5\alpha^{12} \\
& + 188595L^4\alpha^{13} - 49005L^3\alpha^{14} - 15498L^2\alpha^{15} + 8262L\alpha^{16} - 972\alpha^{17}) / \\
& (85171L^{18} + 511026L^{17}\alpha + 225591L^{16}\alpha^2 - 3150739L^{15}\alpha^3 - 3583555L^{14}\alpha^4 \\
& + 7068461L^{13}\alpha^5 + 8927306L^{12}\alpha^6 - 9339499L^{11}\alpha^7 - 9604699L^{10}\alpha^8 \\
& + 8101030L^9\alpha^9 + 4463541L^8\alpha^{10} - 3368349L^7\alpha^{11} - 1026444L^6\alpha^{12} - 6129L^5\alpha^{13} \\
& + 987795L^4\alpha^{14} - 310824L^3\alpha^{15} - 102384L^2\alpha^{16} + 62451L\alpha^{17} - 8019\alpha^{18}) \quad (A.5)
\end{aligned}$$

The derived expression for  $\eta$ , for pinned-guided boundary condition, is given by

$$\begin{aligned}
& \eta = -(20(-5L^2 + \alpha^2)^2 \\
& (48900000L^{19} - 391250000L^{17}\alpha^2 + 366812500L^{16}\alpha^3 + 553400000L^{15}\alpha^4 \\
& - 870000000L^{14}\alpha^5 - 71662500L^{13}\alpha^6 + 695450000L^{12}\alpha^7 - 296600000L^{11}\alpha^8 \\
& - 172118750L^{10}\alpha^9 + 177876500L^9\alpha^{10} - 29350000L^8\alpha^{11} - 24472000L^7\alpha^{12} \\
& + 14047500L^6\alpha^{13} - 2406840L^5\alpha^{14} - 275025L^4\alpha^{15} \\
& + 194056L^3\alpha^{16} - 36030L^2\alpha^{17} + 3132L\alpha^{18} - 108\alpha^{19})) / \\
& (18800953125L^{24} - 147948812500L^{22}\alpha^2 + 128533156250L^{21}\alpha^3 \\
& + 248988306250L^{20}\alpha^4 - 344144687500L^{19}\alpha^5 - 114628978125L^{18}\alpha^6 \\
& + 355622531250L^{17}\alpha^7 - 71640558125L^{16}\alpha^8 - 165701200000L^{15}\alpha^9 \\
& + 95341557500L^{14}\alpha^{10} + 21440472500L^{13}\alpha^{11} - 33688599500L^{12}\alpha^{12} \\
& + 7799345000L^{11}\alpha^{13} + 2084708250L^{10}\alpha^{14} - 1382213250L^9\alpha^{15} \\
& + 441740275L^8\alpha^{16} - 243289500L^7\alpha^{17} + 110922225L^6\alpha^{18} - 23176900L^5\alpha^{19} \\
& - 374990L^4\alpha^{20} + 1229700L^3\alpha^{21} - 262845L^2\alpha^{22} + 24570L\alpha^{23} - 891\alpha^{24}) \quad (A.6)
\end{aligned}$$

The derived expression for  $\eta$ , for fixed-guided boundary condition, is given by

$$\begin{aligned}
& \eta = -(160(-10L^3 + 15L^2\alpha - 7L\alpha^2 + \alpha^3)^2 \\
& (1528125L^{11} - 7131250L^{10}\alpha + 13531875L^9\alpha^2 - 13470000L^8\alpha^3 \\
& + 7420000L^7\alpha^4 - 2199500L^6\alpha^5 + 494500L^5\alpha^6 - 341800L^4\alpha^7 \\
& + 227500L^3\alpha^8 - 77360L^2\alpha^9 + 12960L\alpha^{10} - 864\alpha^{11})) / \\
& (18800953125L^{18} - 142257625000L^{17}\alpha + 486435062500L^{16}\alpha^2 \\
& - 995259512500L^{15}\alpha^3 + 1358358687500L^{14}\alpha^4 - 1304124375000L^{13}\alpha^5 \\
& + 904362862500L^{12}\alpha^6 - 456797400000L^{11}\alpha^7 + 164814030000L^{10}\alpha^8 \\
& - 36505250000L^9\alpha^9 - 2245522000L^8\alpha^{10} + 8036044000L^7\alpha^{11} \\
& - 5355076700L^6\alpha^{12} + 2301922400L^5\alpha^{13} - 690268800L^4\alpha^{14} \\
& + 142894720L^3\alpha^{15} - 19471680L^2\alpha^{16} + 1572480L\alpha^{17} - 57024\alpha^{18}) \quad (A.7)
\end{aligned}$$